

# Toward Rapid, High-Sensitivity, Volume-Constrained Biomarker Quantification and Validation using Backscattering Interferometry

Ian R. Olmsted,<sup>†</sup> Mohamed Hassanein,<sup>‡</sup> Amanda Kussrow,<sup>†</sup> Megan Hoeksema,<sup>‡</sup> Ming Li,<sup>§</sup> Pierre P. Massion,<sup>‡,||,⊥</sup> and Darryl J. Bornhop<sup>\*,†</sup>

<sup>†</sup>Department of Chemistry and the Vanderbilt Institute of Chemical Biology, Vanderbilt University, 4226 Stevenson Center, Nashville, Tennessee 37235, United States

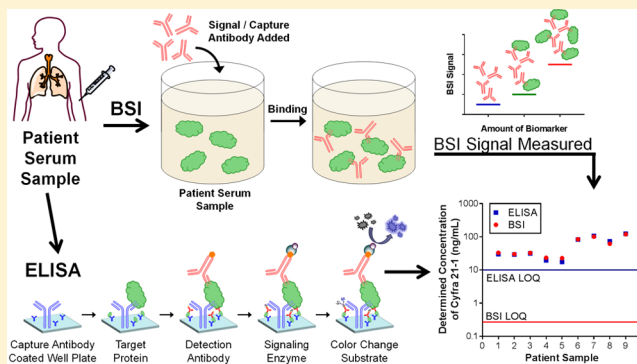
<sup>‡</sup>Division of Allergy, Pulmonary and Critical Care Medicine, Thoracic Program, Vanderbilt Ingram Cancer Center, Department of Medicine, Vanderbilt University School of Medicine, Nashville, Tennessee 37235, United States

<sup>§</sup>Department of Biostatistics, Vanderbilt Ingram Cancer Center, Vanderbilt University School of Medicine Nashville, Tennessee 37235, United States

<sup>||</sup>Department of Cancer Biology, Vanderbilt-Ingram Cancer Center, Vanderbilt University School of Medicine, Nashville, Tennessee 37235, United States

<sup>⊥</sup>Veterans Affairs, Tennessee Valley Healthcare System, Nashville Campus, Nashville, Tennessee 37235, United States

**ABSTRACT:** Realizing personalized medicine, which promises to enable early disease detection, efficient diagnostic staging, and therapeutic efficacy monitoring, hinges on biomarker quantification in patient samples. Yet, the lack of a sensitive technology and assay methodology to rapidly validate biomarker candidates continues to be a bottleneck for clinical translation. In our first direct and quantitative comparison of backscattering interferometry (BSI) to fluorescence sensing by ELISA, we show that BSI could aid in overcoming this limitation. The analytical validation study was performed against ELISA for two biomarkers for lung cancer detection: Cyfra 21-1 and Galectin-7. Spiked serum was used for calibration and comparison of analytical figures of merit, followed by analysis of blinded patient samples. Using the ELISA antibody as the probe chemistry in a mix-and-read assay, BSI provided significantly lower detection limits for spiked serum samples with each of the biomarkers. The limit of quantification (LOQ) for Cyfra-21-1 was measured to be 230 pg/mL for BSI versus 4000 pg/mL for ELISA, and for Galectin-7, it was 13 pg/mL versus 500 pg/mL. The coefficient of variation for 5 day, triplicate determinations was <15% for BSI and <10% for ELISA. The two techniques correlated well, ranging from 3–29% difference for Cyfra 21-1 in a blinded patient sample analysis. The label-free and free-solution operation of BSI allowed for a significant improvement in analysis speed, with greater ease, improved LOQ values, and excellent day-to-day reproducibility. In this unoptimized format, BSI required 5.5-fold less sample quantity needed for ELISA (a 10 point calibration curve measured in triplicate required 36  $\mu$ L of serum for BSI vs 200  $\mu$ L for ELISA). The results indicate that the BSI platform can enable rapid, sensitive analytical validation of serum biomarkers and should significantly impact the validation bottleneck of biomarkers.



The quantification of protein biomarkers at physiologically relevant levels is essential for individualized medicine and early-stage disease diagnostics to be realized. Researchers consider that several factors are impeding the translation of biomarkers into the clinic. Among the major contributors for the clinical translation bottleneck are the intrinsic biological variability in large cohorts of samples for systemic biomarkers, the relatively long development time for assays, and the need for assays with more sensitivity.

Many methods have been developed to detect biomarkers, study pathogenesis, and follow pharmacologic response in cancer, yet they all have limitations with respect to clinical translation. Among the most common methods are ELISA,

bead array technologies, label-free techniques such as surface plasmon resonance (SPR), quartz-crystal microbalance, wave-guided interferometry<sup>1–3</sup> (Table 1), and mass spectrometry (MS).<sup>4,5</sup> Some of these platforms report single-molecule sensitivity<sup>6</sup> and have shown the potential to impact clinical practice.<sup>7</sup> Yet, these techniques have deficiencies with respect to validation, principally related to speed, reproducibility, cost, and/or accessibility.<sup>4</sup> Although MS has been exceedingly valuable in the biomarker discovery phase,<sup>8,9</sup> current

Received: April 14, 2014

Accepted: June 20, 2014

Published: June 20, 2014

Table 1. Comparison of Biomarkers Detection Methods

assay platform	format	detection limit
optical fiber coupler <sup>11</sup>	surface immobilized	10 nM
waveguide techniques <sup>12</sup>	surface immobilized	1 nM
surface plasmon resonance <sup>13,14</sup>	surface immobilized	500 pM (serum), 100pM (buffer)
interferometric techniques <sup>15</sup>	surface immobilized	20 pM (buffer/serum)
ring resonator techniques <sup>16</sup>	surface immobilized	6.5 pM (serum), 3 pM (buffer)
photonic crystal <sup>17</sup>	surface immobilized	800 fM (buffer)
backscattering interferometry	free solution	10 fM
Erenna Singulex <sup>18</sup>	surface immobilized	2fM
single-molecule arrays (Simoa) <sup>6,19</sup>	surface immobilized	200 aM (fluorescent readout)
magnetic nanosensor <sup>20</sup>	surface immobilized	50 aM (nanoparticle amplification)

instrumentation complexity and difficulty with quantification make its use in clinical validation unattractive.<sup>10</sup> Multiplexed MRM/MS targeted assays using stable-isotope-labeled peptide standards for accurate quantitation are showing promise as clinical diagnostic assays, yet complexity and low-throughput remain as challenges. The requirement of other platforms for either surface immobilization and/or labeling steps makes assay development and species validation arduous, slow, and expensive. Therefore, free-solution methods, particularly those that are label-free, represent an attractive alternative to ELISA.

It is true that significant strides have been made toward miniaturizing and multiplexing ELISA.<sup>21–23</sup> Table 1 also illustrates that improving the limit of detection of labeled assays has been possible. One example is the use of electrochemiluminescent assays, which are typically 10-fold more sensitive than the standard fluorescent analogue.<sup>24</sup> Yet these and the other amplification chemistries needed to accomplish femtomolar detection limits carry relatively high costs, long development times, and high failure rates,<sup>24</sup> extending the interval between biomarker discovery and clinical validation. Furthermore, the large sample consumption associated with some of these methods impedes validation of promising biomarkers due to the preciousness of the available banked samples on relevant patient populations.<sup>10,25</sup> As shown from Table 1, backscattering interferometry (BSI) represents the most sensitive label-free method and can give comparable detection limits to fluorescent assays.

In addition to analytical limitations, researchers also consider the intrinsic biological variability in large cohorts of samples to be a major contributor to the clinical translation bottleneck for systemic biomarkers.

As in any assay based on detecting a binding event, the specificity and sensitivity of BSI are impacted by the equilibrium binding affinity,  $K_D$ . In general, the higher the affinity, the lower the potential limit of detection. However, the sensitivity of all interaction-based determinations is impacted by other factors. Fluorescence performance is impacted by quantum efficiencies, and absorbance sensitivity is linked to the molar absorptivity of the analyte. In BSI, the two predominant parameters impacting assay performance are the number of bonds formed (or broken)<sup>26</sup> and the magnitude of change in dipole moment (RI) due to conformation/hydration changes during the binding event.

To test the analytical utility of BSI for biomarker method development and validation, we chose to study two potential biomarkers of lung cancer: one currently in use and one new candidate. Nonsmall cell lung cancer (NSCLC) is the number one cause of cancer mortality among men and women worldwide.<sup>27</sup> In the U.S. alone, lung cancer kills more men

and women than colorectal, prostate, and breast cancer combined.<sup>28</sup> Despite advances in diagnostic and treatment strategies over the past decade, the prognosis of patients with lung cancer remains poor. Seventy percent of patients are diagnosed at an advanced stage,<sup>28</sup> primarily due to the lack of sensitive and specific detection methods, with an overall 5 year survival rate of 15%.<sup>29,30</sup> In response to this critical need for a reliable early detection method, the search for early stage noninvasive diagnostic strategies for lung cancer detection has intensified.<sup>31</sup> Computed tomography (CT) is the most common method used for diagnosing lung cancer, but CT has limitations. Lung nodules of indeterminate significance are discovered in over 25% of the individuals screened with CT.<sup>32</sup> As revealed by expensive and invasive diagnostic tests used to discriminate these lesions, 96% of these hard to distinguish nodules are benign.<sup>33</sup> The development of a simple, rapid, specific, noninvasive, and clinically relevant diagnostic tool would improve early lung cancer detection, reduce the need for unnecessary biopsies, and enable early treatment.

We hypothesized that BSI,<sup>34,35</sup> a simple, isothermal, highly sensitive free-solution, label- and enzyme-free technology, compatible with complex matrices could provide improved sensitivity for protein biomarker analysis and reduce the assay development bottleneck encountered with labeled and/or tethered assays. BSI is based on a unique resonant cavity interferometric approach that can give femtomolar sensitivity without labels, in submicroliter sample volumes. Additionally, the BSI signal transduction mechanism makes it highly modular and not limited by the mass of the target or probe.<sup>36</sup> Studies have shown that ligand–receptor binding induced conformational, solvation/desolvation, molecular polarizability, and dipole moment changes correlate with refractive index (RI)-induced fringe shifts observed in BSI.<sup>26,28</sup> The ability to measure these properties allows a wide array of interactions (antibodies to DNA to small molecules) to be quantified with a large range of affinities ( $\mu\text{M}$  to pM) regardless of the mass of the interacting species.<sup>26,34,37–39</sup> Because RI changes may arise from molecular interactions unrelated to target binding, suitable blanks and controls must be prepared to ensure that the measured changes reflect an actual binding event. In addition, temperature control is employed to constrain background noise arising from thermal fluctuations.

To test our hypothesis, we compared the performance of BSI to that of the commercially available ELISA for the quantification of two NSCLC protein biomarkers. One was Cyfra 21-1, which is currently used in the clinic to stage patient disease state. The other was a candidate biomarker, Galectin-7, identified from a shotgun proteomics screen.<sup>40</sup> Limits of quantification (LOQ) for the respective assays were determined

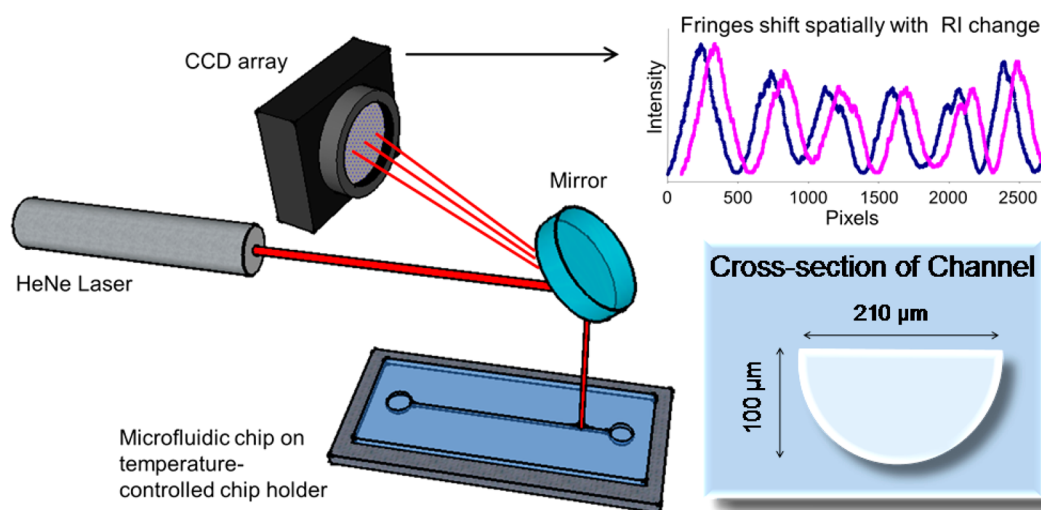


**Figure 1.** BSI experimental setup. The laser is directed onto the microfluidic chip by a mirror that also serves to direct the interference fringes on the detector. As shown, the channel in the chip has a near semicircular cross section. When the fluid RI changes in the channel the interference fringes shift spatially.

in spiked human serum. Next, a small set of blinded clinical samples was evaluated. The results indicate that BSI has the potential to rapidly and effectively quantify biomarkers in serum or plasma with significant improvement in sensitivity compared to ELISA, opening an avenue for rapid biomarker validation.

## EXPERIMENTAL SECTION

BSI has been described extensively in previous publications.<sup>36,41,42</sup> Briefly, the instrument is comprised of a helium–neon (HeNe) laser, a mirror, a microfluidic chip, and a linear charged-coupled device (CCD) detector (Figure 1). The sample is introduced into the microfluidic chip, which has a near-semicircular cross section, configured to create a resonance cavity with a long effective path length. The incident coherent light is converted into an interferometric fringe pattern, which is captured by the CCD camera. Fourier analysis is used to determine the phase change (in radians),<sup>43</sup> which is a quantitative measure of spatial position of the fringes due to changes in refractive index (RI). These RI changes have been shown to correlate with ligand–receptor binding<sup>36,41</sup> and are used to quantify molecular interactions<sup>36</sup> with subpicomolar sensitivity and a large dynamic range.<sup>34,36</sup>

A calibration curve was constructed for each biomarker in order to determine the BSI lower limit of detection. All reagents used were from commercial ELISA kits (DRG International and DuoSet for Cyfra 21-1 and Galectin-7 assays, respectively). Increasing concentrations of recombinant protein [0, 0.156, 0.312, 0.625, 1.25, 2.5, 5, and 10 ng/mL for Cyfra 21-1; 0, 0.41, 0.82, 1.64, 3.28, 6.56, 13.12, 26.25, and 52.5 ng/mL for Galectin-7 (single antibody calibration); and 0, 0.02, 0.04, 0.08, 0.156, 0.312, 0.625, and 1.25 ng/mL for Galectin (two antibody calibration)] spiked in 20% human serum were incubated with a constant concentration of antibody for 1 h at room temperature to allow for binding equilibrium. A series of blanks were similarly prepared, using buffer in lieu of antibody. At equilibrium, 1  $\mu$ L of sample was injected into the BSI channel and measured for 30 s. The corresponding blank was immediately measured after the sample and subtracted from the sample signal as the background. All samples and blanks were

prepared fresh daily, then sequentially measured in triplicate daily for 5 days.

Cyfra 21-1 and Galectin-7 calibration curves data were fit to a four parameters logistic model and plotted as a function of analyte concentrations. Curve fit functions were chosen on the basis of the best  $R^2$  value using GraphPad Prism software package.

Calibration curves for both biomarkers were also constructed as a benchmark with spiked 20% human serum using commercial ELISA kits (DRG International and DuoSet for Cyfra 21-1 and Galectin-7 assays, respectively). The ELISA calibration curve was created using triplicate determinations, following the manufacturer's recommended procedure. Lower limits of detection were calculated by determining the lowest concentration at which the signal-to-noise ratio was  $\geq 5$ . An alternative calculation was performed using the following equation:

$$\text{LOQ} = 3\sigma / \text{initial slope}$$

where  $\sigma$  = the average standard deviation of all 15 trials run over 5 separate days. The initial slope was calculated by taking the linear regression of the lowest four concentrations measured. The results of both methods were in close agreement.

Serum samples were collected from individuals with lung cancer and controls from the biorepository of the thoracic program at the Vanderbilt Ingram Cancer Center. Serum samples were prepared following a previously described standard operating procedure, aliquoted, and stored at  $-80^\circ\text{C}$  until analysis.<sup>40</sup> For Galectin-7 analysis, eight samples were from patients with NSCLC histology (stages IA–IIIA) of either squamous cell carcinoma (SCC,  $N = 2$ ) or adenocarcinoma subtypes (ADC,  $N = 2$ ) and controls from individuals with no sign of lung cancer ( $N = 4$ ) (Table 2). Control individuals were defined as having no evidence of lung cancer at their 1 year follow-up exam. For Cyfra 21-1 analysis, 10 samples were from controls ( $N = 5$ ) and individuals with SCC ( $N = 5$ ), as outlined in Table 2. Patient serum samples were from individuals matched for age, gender, and smoking history. Patient samples were prepared at a 1:5 dilution with PBS buffer and as described previously for the spiked samples. Patient serum



Table 2. Summary of Patient Samples Characteristics

sample	gender	age	cancer	smoking status	pack years
Galectin-7 patients					
1	male	58	none	never smoker	0
2	male	48	none	ex-smoker	34.5
3	female	66	ADC -stage IB	ex-smoker	7.5
4	male	84	SCC -stage IA	ex-smoker	40
5	female	76	none	ex-smoker	56
6	female	64	none	ex-smoker	40
7	female	70	ADC -stage IB	current smoker	75
8	male	64	SCC -stage IA	ex-smoker	20
Cyfra 21-1 patients					
1	male	46	none	never smoker	0
2	male	56	none	ex-smoker	100
3	male	44	none	current smoker	15
4	female	67	none	ex-smoker	15
5	male	70	none	current smoker	29
6	male	62	SCC -stage IV	current smoker	25
7	male	50	SCC -stage IIIB	ex-smoker	162
8	male	63	SCC -stage IIIB	ex-smoker	72
9	female	87	SCC -stage IV	ex-smoker	70
10	male	68	SCC -stage IV	ex-smoker	40

samples were analyzed using a commercial ELISA kit that was performed according to the manufacturer's specified procedure. The institutional review board at Vanderbilt University approved these human studies.

## RESULTS AND DISCUSSION

Here Cyfra 21-1 and Galectin-7 were employed to evaluate the potential to use BSI as a mix-and-read analysis method in biomarker validation. It is noteworthy that this research represents an analytical *assay* validation study and not a clinical validation of either the biomarker or the assay. The importance of this research is the potential for BSI to speed biomarker *assay methods* development, provide improved performance over ELISA, and offer an alternative for solving the current biomarker analytical validation bottleneck.

In our proof-of-concept experiment, we compared the performance of BSI and ELISA with analysis of human serum and plasma spiked with the protein biomarkers of interest. In all of the studies reported here, we used the probe chemistry (antibody[s]) from the ELISA kit for the BSI assay. Using our free-solution, mix-and-read approach, we achieved excellent sensitivity and reproducibility by spiking human serum with

Cyfra 21-1. For example, Figure 2A presents the calibration curves for BSI and ELISA, showing a more than a 17.3-fold increase in sensitivity. The plot also shows that the assay was highly reproducible over a 5 day period.

Cyfra 21-1 is currently a NSCLC blood-based candidate biomarker with a concentration that has some clinical utility in that it correlates with disease progression,<sup>44–47</sup> but its diagnostic utility has been restricted by the low constitutive expression in healthy individuals (2.4 ng/mL),<sup>45</sup> a value which is well below the reported ELISA detection limit of 10 ng/mL.<sup>48</sup> As with C-reactive protein (CRP), discussed below, we believe a 10–20-fold improvement in the LOQ has the potential to expand the diagnostic value of the Cyfra 21-1 biomarker. Here we show that one advantage of BSI is an improved LOQ for Cyfra 21-1.

Galectin-7 was recently identified by shotgun proteomics and has been reported as an NSCLC tissue marker<sup>40</sup> with the potential to serve as a diagnostic target. As with many potential targets, Galectin-7 has yet to be validated as a useful serum or plasma NSCLC biomarker, principally due to the time-consuming process needed to develop a biomarker assay prior to clinical validation. The analytical discovery and validation process currently requires the identification of two antibodies, successful fluorescent labeling, and capture probe immobilization chemistry to be implemented prior to analytical testing. It is only after this arduous process is completed that the resulting assay can be validated, first with respect to analytical performance and then in a clinical setting. Recently, we found that even after a great deal of optimization, the ELISA kit developed for Galectin-7 was unable to quantify the target in low-level-expressing patients. Thus, even though tissue studies<sup>40</sup> suggested it should serve as an early disease marker, it was impossible to determine the value of the protein as a serum biomarker with the ELISA test. Here we show that we could rapidly develop a BSI assay that had significantly improved detection limits for Galectin-7.

Figure 2B shows that overall the calibration curves for BSI and ELISA show a more than 38-fold increase in sensitivity. The LOQ for BSI was about 13-fold better than for ELISA (39 pg/mL shown in the blue trace vs 500 pg/mL shown in the green trace) using the detection antibody. Capitalizing on our recent observation that the BSI signal is proportional not only to the quantity of interacting species leading to conformation and hydration changes upon binding but also to the number of binding events within a molecule, we simply added the capture

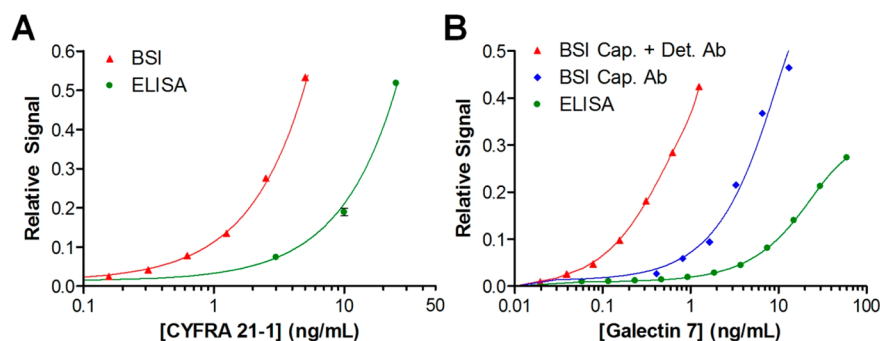


**Figure 2.** (A) Calibration curves for BSI with Cyfra 21-1 spiked into serum (red triangles) and for ELISA in spiked serum (green circles). (B) Calibration curves for Galectin-7 spiked serum show that the BSI LOQ (blue diamonds) is better than for ELISA (green circles) and is improved by using both the detection and capture antibodies in the assay (red triangles). Error bars on both plots represent the standard deviation for repeat triplicate determinations over a 5 day period.

antibody to the assay to improve sensitivity.<sup>26</sup> The use of multiple probes (or even different types) is predicted to improve the LOQ and potentially increase specificity. Figure 2B illustrates the significant performance improvement of BSI performance by using both the capture and detection antibody from a DuoSet human Galectin-7 ELISA kit. In this case, comparison of the red trace to the blue trace in Figure 2B illustrates a 3-fold improvement in LOQ for Galectin-7 in spiked serum by simply employing both the capture and detection antibodies (13 pg/mL vs 39 pg/mL). The data in this figure represents triplicate determinations performed on 5 subsequent days ( $n = 15$ ). Although not demonstrated here, we have shown with Bock and Tasset aptamers to thrombin that BSI is unique in that careful selection of the binding pair and order of addition can increase both the affinity and the S/N of the measurement.<sup>38</sup>

Table 3 summarizes our ELISA-BSI comparison results for the two biomarkers studied. Over a 5 day period, the BSI LOQ

**Table 3. Limit of Quantification (LOQ) and Coefficient of Variation for BSI and ELISA assays<sup>a</sup>**

	LOQ (pg/mL)		% CV at LOQ		LOQ improvement
	BSI	ELISA	BSI	ELISA	
Cyfra 21-1	230	4000 <sup>b</sup>	14.7%	9.0%	17.3-fold
Galectin-7	13	500	14.8%	7.1%	38.5-fold

<sup>a</sup>LOQ calculated by  $3\sigma/\text{slope}$  ( $\sigma$  = average standard deviation over 15 trials) % CV calculated by standard deviation over 15 trials/mean signal concentration. <sup>b</sup>Manufacturer's quoted LOQ is 10 000 pg/mL.

was 38-fold better than ELISA for Galectin-7 and 17-fold better for Cyfra 21-1. The coefficient of variation (CV) was less than 15% at the LOQ for all BSI assays, showing excellent assay precision and reproducibility using a research laboratory instrument.

It is possible to further improve the ELISA detection limits using methods that employ additional signal amplification and/or noise reduction methods. For example Lee et al. recently reported the quantification of Cyfra 21-1 using Luminex at levels as low as 0.01 ng/mL.<sup>49</sup> They present data for healthy patients ranging from 0.01 to 0.73 ng/mL and cancer patients having 0.66 to 2.4 ng/mL, yet the manufacturer reports a minimum detection concentration at 2 times the standard deviation of 0.059 ng/mL. Here we use a more conservative measure of performance, the LOQ, which is based on 3 times

the standard deviation of the assay run over 5 days. Comparing BSI to the bead-based assay is difficult in this case, but the BSI LOQ (not the LOD at  $2\sigma$ ) exhibits >1.5-fold improvement and is performed as a free-solution and label-free method.<sup>49,50</sup> Electrochemiluminescence assays have demonstrated detection limits comparable to ours reported here,<sup>25,49,50</sup> yet these assays are expensive and require substantial chemical complexity in both the assay discovery and analytical validation phase.

Next, we demonstrated that BSI can be used to quantify these biomarkers in patient samples in a blinded fashion, using a small set of previously characterized samples spanning a range of lung cancer stages (see Table 2). As with the spiked samples, serum was diluted 1:5 with PBS buffer, split into aliquots, and analyzed individually for Cyfra 21-1 and Galectin-7. A 1:10 dilution of antibody, (1  $\mu$ L of antibody solution/9  $\mu$ L of serum) was incubated at room temperature for 1 h. A reference sample of the same serum dilution with buffer was run in tandem with each patient sample to correct for bulk RI changes inherent to the sample. The difference in shift between the sample and the reference was recorded, and the concentration of the biomarker in each patient sample was determined using the appropriate response curve (Figures 2A,B) for Cyfra 21-1 or Galectin-7. Again, assays were performed in triplicate daily for 5 days ( $n = 15$ ).

Figure 3A shows BSI and ELISA results plotted on a log-scale versus patient number for the quantification of Cyfra 21-1. In this set, there were five samples from patients with disease (cases) and five from patients without (controls). Figure 3B shows the data on an expanded scale, covering slightly more than 1 decade in concentration. At this scale, the error bars for the 15 replicate determinations become visible, as well as the difference in Cyfra 21-1 concentration determined by the two methods. Overall, the BSI correlated with ELISA measurements (3–29% difference), with the cases and controls segregating as expected (see Figure 5A). In this case, we chose five patients with relatively advanced disease (four at stage IV and one at stage IIIA–IIIB) and five controls derived from patients that do not currently have detectable disease. Yet, as shown by the LOQ cutoff lines on the plot, the threshold for quantifying the biomarker with confidence for the two methodologies is considerably different. This enhanced sensitivity could allow for more accurate stratification of patients with existing NSCLC. As discussed below, because Cyfra 21-1 has relatively low constitutive expression (near the LOQ for ELISA), this sensitivity advantage for quantifying Cyfra 21-1 in serum

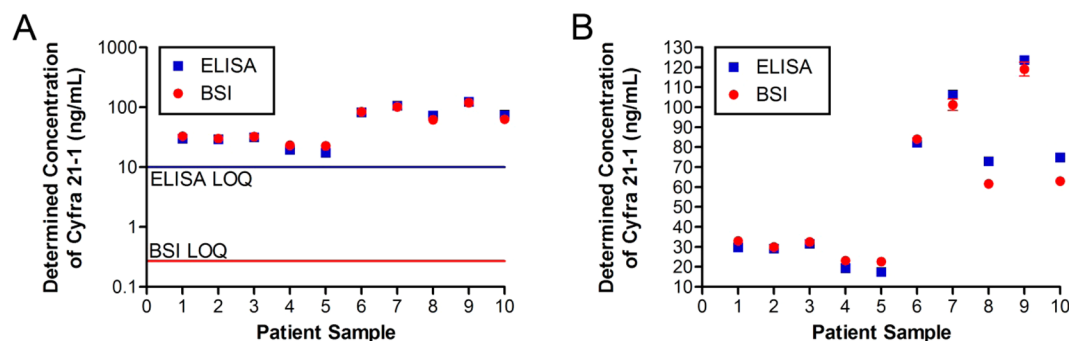


**Figure 3.** Determination of Cyfra 21-1 concentration in human patient serum samples using BSI and ELISA and the calibration plots shown in Figure 2. (A) Cyfra 21-1 concentrations determined by BSI and ELISA plotted on a log scale and compared to the LOQ for each method. (B) Expanded y-axis illustrates the similarities of the measured Cyfra 21-1 concentration for both methods. Error bars on both plots represent 15 independent measurements performed over 5 days.

could allow for earlier detection of disease and/or enable monitoring therapeutic response in NSCLC.<sup>40</sup>

Our patient sample analysis for Galectin-7 (Figure 5) was less conclusive with respect to case/control discrimination and calls into question the diagnostic potential of this biomarker. Tissue ELISA results suggested Galectin-7 was a promising biomarker of lung cancer (data not shown). Yet here, as with other biomarkers, the tissue and serum data do not correlate. Galectin-7 may still have clinical utility when this sample type is available, yet our results indicate that serum levels are not predictive of the presence of disease.

The findings illustrate several advantages of BSI in the biomarker validation phase. First, the high sensitivity of BSI, with all Galectin-7 samples being within the LOQ, provides reasonable confidence that poor assay performance is not the discordance of the tissue–serum results. Second, mix-and-read operation allowed for us to rapidly establish in a small but relevant patient population that there was no correlation between the serum and tissue biomarker expression levels. This is a critical step in validation, providing a check point before investing time and resources on further assay development. Third, BSI can be used with existing antibodies (probe chemistry) to provide a significantly improved LOQ over the conventional fluorescent assay.

Figure 4 illustrates the BSI and ELISA results for serum correlate in general; however, they show differences of as much

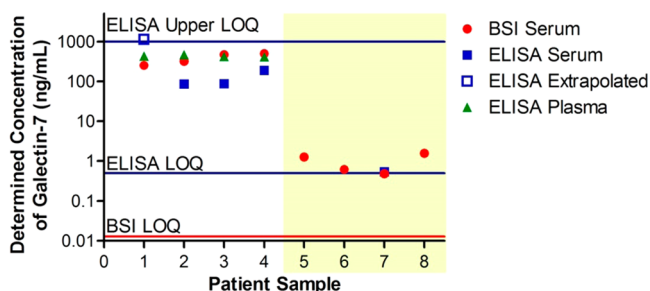


**Figure 4.** Determination of Galectin-7 concentration in human patient serum samples using BSI and ELISA and the calibration plots shown in Figure 2. BSI was able to quantify the Galectin-7 concentration in all eight patient serum samples, yet half of these samples have a biomarker concentration below the ELISA limit of detection (highlighted in yellow box). Error bars on the plots represent 15 independent measurements performed over 5 days.

as 40-fold. Yet, the ELISA plasma results correlate well with the BSI serum values. It is also important to note that the serum versus plasma ELISA results also exhibit differences approaching 50-fold, with improved assay performance in serum. Currently, we are investigating the source of the disparity between these measurements, and although not within the scope of this report, we hypothesize that a combination of chemical and localized environmental factors may be the culprits.

The majority of protein detection platforms recognize a specific binding event to a target molecule, requiring both a signal transducer and immobilization of the probe. This is not the case with BSI, which is a label-free and free-solution platform, compatible with many probes, targets, and events. ELISAs, protein microarrays,<sup>51–54</sup> and even quantum dot<sup>55</sup> platforms have a readout that is either fluorescent or colorimetric. Matrix autofluorescence or intrinsic absorption of the samples or reagents can be a major limiting factor in

these methods. pH and ionic strength can also impact an assay, particularly one performed in the tethered mode. Just a 0.14 M salt solution (similar to human serum) has been shown to have sufficient Debye forces to shield nanowires from detecting protein binding events.<sup>56</sup> In our own<sup>57</sup> and collaborators' laboratories,<sup>39</sup> we have illustrated that ligand binding in surface-immobilized formats are inherently susceptible to slight changes in the binding environment and that BSI can discriminate these perturbations.<sup>57</sup> Even though LOQ performance of BSI is impacted by environment (Figure 2A) for Cyfra 21-1, using the *same matrix* for the reference/control as we do in BSI provides some inherent immunity to these influences.<sup>34,35</sup> In theory, as long as the measurements are performed within the dynamic operation range of the assay quantification accuracy should be maintained. Studies are currently underway to confirm our hypothesis and address these disparities.

The LOQ is critical to the successful deployment of a predictive biomarker assay.<sup>4,58–60</sup> Figures 2–4 all show that BSI has a significant LOQ advantage over standard ELISA, allowing for the analysis of four Galectin-7 samples that could not be quantified with the fluorescent method. Three of these patient samples had a target concentration well below the LOQ and one of them was near the high end of the dynamic range. It is in this lower region that we believe the high sensitivity of BSI will provide the opportunity to expand the use of biomarker assays in the clinic, as was the case for hsCRP (high-sensitivity C-reactive protein assay).<sup>61–63</sup>

The intraclass correlation coefficient (ICC), a reliability index, was calculated to evaluate the reproducibility of the BSI measurements for both Cyfra 21-1 and Galectin-7, and this determination is shown in Figure 5. The ICC was determined to be 0.93 for Cyfra and 0.96 for Galectin, demonstrating that the variation of the measurements on the same sample is significantly lower than the variation of the measurement of two different samples, an indication that the measurement has a high degree of accuracy. These data also illustrate a clear separation between case and control samples for Cyfra 21-1, as expected for this biomarker. However, the patient samples analyzed for Galectin-7 show a much wider range of concentrations, regardless of cancer stage (Table 2), and even though the patient sample sets studied were relatively small, these results bring into question the value of this protein as a circulating biomarker of NSCLC. For both ELISA and BSI, Galectin-7 was present in serum at the levels necessary to provide the sensitivity and selectivity to accurately discern between cases and controls. As noted above, this biomarker likely represents an example where there is a poor correlation between tissue expression and circulating levels in serum.

To illustrate the potential of our approach, we cite an analogy to the development of the CRP assay. The CRP assay was discovered many years ago and was used on a limited basis as an inflammation marker. Yet, recently it has become a standard clinical measurement for cardiovascular disease (CVD),<sup>62</sup> which is due in great part to a dramatic performance improvement (20-fold) afforded by the hsCRP assay. It was the hsCRP assay that allowed the demonstration of a correlation for this biomarker and CVD.<sup>62</sup> Higher sensitivity or improved LOQ performance enabled the quantification of this rather abundant protein at very low concentrations,<sup>61,62</sup> and the demonstration of its presence correlates well with various degrees of CVD, providing a standard of care for risk assessment.<sup>63,64</sup> Another example has been shown with PSA.<sup>7,65</sup> In this case, the fifth-generation PSA assay capitalizes on



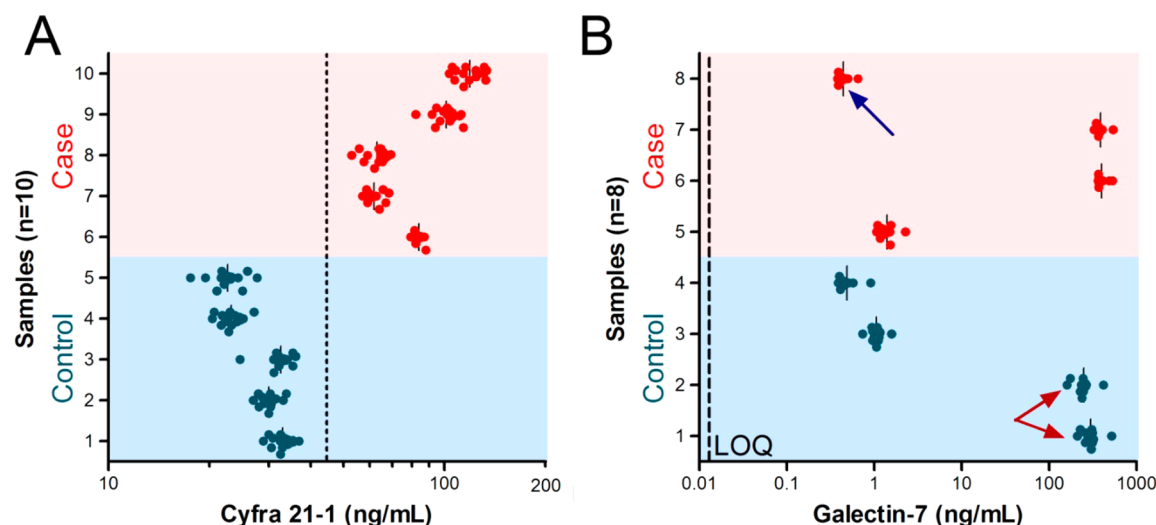


**Figure 5.** Intraclass correlation coefficient (ICC) plots for BSI assays. (A) Raw patient sample data for Cyfra 21-1 measured each day in triplicate for 5 separate days. The 15 measurements (dots) of the control samples (blue) and the case samples (red) show a clear differentiation between disease states seen by the dotted line. (B) Raw patient sample data for Galectin-7 measured each day in triplicate for 5 days. Although the 15 measurements (dots) of all the samples are well above the BSI LOQ (dashed line), the control samples (blue) and the case samples (red) do not show a differentiation. Red and blue arrows point to patient samples that put into question the validity of this biomarker.

amplified ELISA and femtoliter volumes to approach single-molecule detection and shows promise in providing additional clinical insights about recurrence for prostate cancer patients.

Assay speed, simplicity, sensitivity, and cost significantly impacts the effectiveness of biomarker validation. Further, the precious nature of the samples requires that sample consumption be minimized. The entire assay was performed on 5.5-fold less sample volume than that required by ELISA (10 point calibration curve measured in triplicate required 36  $\mu\text{L}$  of serum for BSI vs 200  $\mu\text{L}$  for ELISA), and optimization may reduce this volume along with reduced reagent consumption. If existing ELISA kits are available and used, then the speed of the actual determination is similar. Both methods require incubation, but BSI does not demand numerous rinsing steps, as in the sandwich assay and plate reading steps required for ELISA, thus significantly speeding the process. Dose–response curves are constructed by simply incubating increasing concentrations of the recombinant protein spiked into human serum with 100 ng/mL of the antibody from an ELISA kit. With respect to clinical validation, a major bottleneck continues to be the time needed to perform analytical validation (development and characterization) of the assay before the necessary step of an expansive set of patient samples being fully characterized. Often, as with Galectin-7, after weeks to months of development, the final fluorescent assay performance negates use for a clinical validation. The mix-and-read and label-free nature of BSI allows numerous probe chemistries (antibodies, aptamers, and small molecules) to be characterized and optimized in just hours to days. If necessary, BSI can also be used in the tethered format and without the inherent mass sensitivity limitations encountered with SPR and similar methods. Thus, when desirable, we can rapidly develop an assay in free solution and then translate it to the clinical setting in a disposable chip format without concern that changing the format will impact performance.

## CONCLUSIONS

Here we demonstrated that BSI enables the quantification of NSCLC biomarkers in complex biological matrices at

concentrations that are up to 40-fold lower than commonly used assays (Table 3). BSI also characterized patient serum samples in good agreement with results by the current gold standard in disease diagnosis (ELISA). The free-solution and label-free assay format allows optimization in hours to days, instead of weeks or months, expediting the biomarker validation process. In addition, BSI requires less sample volume, allowing a wider array of biomarkers and probes to be investigated during the initial screening phase of the validation process. In our small set of blinded patient samples, BSI compared well with ELISA. Our ongoing BSI performance optimization efforts<sup>26</sup> indicates new probes such as aptamers have potential to enhance NSCLC biomarker quantification, whereas our exploration of two promising sample introduction strategies shows the promise of volume-constrained increased throughput in BSI. One approach is optical, and the other capitalizes on microfluidics. Taken collectively, it is possible that the high sensitivity and simplicity of the BSI assay will expedite the validation of biomarkers for disease diagnosis, risk assessment, and response to therapy.

## AUTHOR INFORMATION

### Corresponding Author

\*E-mail: darryl.bornhop@vanderbilt.edu.

### Notes

The authors declare the following competing financial interest(s): D.J.B. and A.K. have a financial interest in a company that is commercializing BSI. The other authors declare that they have no competing financial interests.

## ACKNOWLEDGMENTS

The authors thank the following funding sources for support of this work: The NSF (Grant CHE-0848788) awarded to D.J.B., NCI EDRN CA152662, and SPORE in lung cancer CA90949 awarded to P.P.M. Dr. M. Sexton is acknowledged for manuscript editing. D.J.B. and A.K. have a financial interest in a company that is commercializing BSI. The other authors declare that they have no competing financial interests.

## REFERENCES

- (1) Brosinger, F.; Freimuth, H.; Lacher, M.; Ehrfeld, W.; Gedig, E.; Katerkamp, A.; Spener, F.; Cammann, K. *Sens. Actuators, B* **1997**, *44*, 350–355.
- (2) Goh, J. B.; Loo, R. W.; Goh, M. C. *Sens. Actuators, B* **2005**, *106*, 243–248.
- (3) Ymeti, A.; Kanger, J. S.; Greve, J.; Lambeck, P. V.; Wijn, R.; Heideman, R. G. *Appl. Opt.* **2003**, *42*, 5649–5660.
- (4) Hori, S. S.; Gambhir, S. S. *Sci. Transl. Med.* **2011**, *3*, 109–116.
- (5) Whiteaker, J. R.; Lin, C. W.; Kennedy, J.; Hou, L. M.; Trute, M.; Sokal, L.; Yan, P.; Schoenherr, R. M.; Zhao, L.; Voytovich, U. J.; Kelly-Spratt, K. S.; Krasnoselsky, A.; Gafken, P. R.; Hogan, J. M.; Jones, L. A.; Wang, P.; Amon, L.; Chodosh, L. A.; Nelson, P. S.; McIntosh, M. W.; Kemp, C. J.; Paulovich, A. G. *Nat. Biotechnol.* **2011**, *29*, 625–634.
- (6) Rissin, D. M.; Kan, C. W.; Song, L. N.; Rivnak, A. J.; Fishburn, M. W.; Shao, Q. C.; Piech, T.; Ferrell, E. P.; Meyer, R. E.; Campbell, T. G.; Fournier, D. R.; Duffy, D. C. *Lab Chip* **2013**, *13*, 2902–2911.
- (7) Wilson, D. H.; Hanlon, D. W.; Provuncher, G. K.; Chang, L.; Song, L. N.; Patel, P. P.; Ferrell, E. P.; Lepor, H.; Partin, A. W.; Chan, D. W.; Sokoll, L. J.; Cheli, C. D.; Thiel, R. P.; Fournier, D. R.; Duffy, D. C. *Clin. Chem.* **2011**, *57*, 1712–1721.
- (8) Applied Biosystems. <http://www.appliedbiosystems.com> (Accessed 12/22/2013).
- (9) Mischak, H.; Schanstra, J. P. *Proteomics. Clin. Appl.* **2011**, *5*, 9–23.
- (10) Diamandis, E. P. *J. Intern. Med.* **2012**, *272*, 620–620.
- (11) Tazawa, H.; Kanie, T.; Katayama, M. *Appl. Phys. Lett.* **2007**, *91*, 113091.
- (12) Cunningham, B. T.; Laing, L. *Expert Rev. Proteomics* **2006**, *3*, 271–281.
- (13) Lee, H. J.; Nedelkov, D.; Corn, R. M. *Anal. Chem.* **2006**, *78*, 6504–6510.
- (14) Teramura, Y.; Iwata, H. *Anal. Biochem.* **2007**, *365*, 201–207.
- (15) Fan, X. D.; White, I. M.; Shopoua, S. I.; Zhu, H. Y.; Suter, J. D.; Sun, Y. Z. *Anal. Chim. Acta* **2008**, *620*, 8–26.
- (16) Luchansky, M. S.; Bailey, R. C. *Anal. Chem.* **2010**, *82*, 1975–1981.
- (17) Huang, C. S.; Chaudhery, V.; Pokhriyal, A.; George, S.; Polans, J.; Lu, M.; Tan, R. M.; Zangar, R. C.; Cunningham, B. T. *Anal. Chem.* **2012**, *84*, 1126–1133.
- (18) Shukla, R.; Santoro, J.; Bender, F. C.; Laterza, O. F. *J. Immunol. Methods* **2013**, *390*, 30–34.
- (19) Rissin, D. M.; Kan, C. W.; Campbell, T. G.; Howes, S. C.; Fournier, D. R.; Song, L.; Piech, T.; Patel, P. P.; Chang, L.; Rivnak, A. J.; Ferrell, E. P.; Randall, J. D.; Provuncher, G. K.; Walt, D. R.; Duffy, D. C. *Nat. Biotechnol.* **2010**, *28*, 595–599.
- (20) Gaster, R. S.; Hall, D. A.; Nielsen, C. H.; Osterfeld, S. J.; Yu, H.; Mach, K. E.; Wilson, R. J.; Murrmann, B.; Liao, J. C.; Gambhir, S. S.; Wang, S. X. *Nat. Med.* **2009**, *15*, 1327.
- (21) Wang, J.; Ahmad, H.; Ma, C.; Shi, Q. H.; Vermesh, O.; Vermesh, U.; Heath, J. *Lab Chip* **2010**, *10*, 3157–3162.
- (22) Fan, R.; Vermesh, O.; Srivastava, A.; Yen, B. K. H.; Qin, L. D.; Ahmad, H.; Kwong, G. A.; Liu, C. C.; Gould, J.; Hood, L.; Heath, J. R. *Nat. Biotechnol.* **2008**, *26*, 1373–1378.
- (23) Garcia-Cordero, J. L.; Maerkl, S. J. *Lab Chip* **2014**, DOI: 10.1039/c3lc51153g.
- (24) Muzyka, K. *Biosens. Bioelectron.* **2014**, *54*, 393–407.
- (25) Sanchez-Carbayo, M.; Herrero, E.; Megias, J.; Mira, A.; Soria, F. *J. Urology* **1999**, *162*, 1951–1956.
- (26) Adams, N. M.; Olmsted, I. R.; Haselton, F. R.; Bornhop, D. J.; Wright, D. W. *Nucleic Acids Res.* **2013**, *41*, e103.
- (27) Jemal, A. *Lancet* **2012**, *380*, 1797–1799.
- (28) Parkin, D. M.; Bray, F.; Ferlay, J.; Pisani, P. *Ca-Cancer J. Clin.* **2005**, *55*, 74–108.
- (29) Hoffman, P. C.; Mauer, A. M.; Vokes, E. E. *Lancet* **2000**, *355*, 479–485.
- (30) Schwartz, A. G.; Prysak, G. M.; Bock, C. H.; Cote, M. L. *Carcinogenesis* **2007**, *28*, 507–518.
- (31) Hassanein, M.; Callison, J. C.; Callaway-Lane, C.; Aldrich, M. C.; Grogan, E. L.; Massion, P. P. *Cancer Prev. Res.* **2012**, *5*, 992–1006.
- (32) Aberle, D. R.; Adams, A. M.; Berg, C. D.; Black, W. C.; Clapp, J. D.; Fagerstrom, R. M.; Gareen, I. F.; Gatsonis, C.; Marcus, P. M.; Sicks, J. D.; Team, N. L. S. T. R. N. *Engl. J. Med.* **2011**, *365*, 395–409.
- (33) MacMahon, H.; Austin, J. H. M.; Gamsu, G.; Herold, C. J.; Jett, J. R.; Naidich, D. P.; Patz, E. F.; Swensen, S. J. *Radiology* **2005**, *237*, 395–400.
- (34) Baksh, M. M.; Kussrow, A. K.; Mileni, M.; Finn, M. G.; Bornhop, D. J. *Nat. Biotechnol.* **2011**, *29*, 357–360.
- (35) Kussrow, A.; Enders, C. S.; Castro, A. R.; Cox, D. L.; Ballard, R. C.; Bornhop, D. J. *Analyst* **2010**, *135*, 1535–1537.
- (36) Bornhop, D. J.; Latham, J. C.; Kussrow, A.; Markov, D. A.; Jones, R. D.; Sorensen, H. S. *Science* **2007**, *317*, 1732–1736.
- (37) Kussrow, A.; Enders, C. S.; Bornhop, D. J. *Anal. Chem.* **2012**, *84*, 779–792.
- (38) Olmsted, I. R.; Xiao, Y.; Cho, M.; Csordas, A. T.; Sheehan, J. H.; Meiler, J.; Soh, H. T.; Bornhop, D. J. *Anal. Chem.* **2011**, *83*, 8867–8870.
- (39) Pesciotta, E. N.; Bornhop, D. J.; Flowers, R. A. *Chem. - Asian J.* **2011**, *6*, 70–73.
- (40) Kikuchi, T.; Hassanein, M.; Amann, J. M.; Liu, Q. F.; Slebos, R. J. C.; Rahman, S. M. J.; Kaufman, J. M.; Zhang, X.; Hoeksema, M. D.; Harris, B. K.; Li, M.; Shyr, Y.; Gonzalez, A. L.; Zimmerman, L. J.; Liebler, D. C.; Massion, P. P.; Carbone, D. P. *Mol. Cell. Proteomics* **2012**, *11*, 916–932.
- (41) Kussrow, A.; Kaltgrad, E.; Wolfenden, M. L.; Cloninger, M. J.; Finn, M. G.; Bornhop, D. J. *Anal. Chem.* **2009**, *81*, 4889–4897.
- (42) Markov, D. A.; Swinney, K.; Bornhop, D. J. *J. Am. Chem. Soc.* **2004**, *126*, 16659–16664.
- (43) Markov, D.; Begari, D.; Bornhop, D. J. *Anal. Chem.* **2002**, *74*, 5438–5441.
- (44) Molina, R.; Filella, X.; Auge, J. M.; Fuentes, R.; Bover, I.; Rifa, J.; Moreno, V.; Canals, E.; Vinolas, N.; Marquez, A.; Barreiro, E.; Borrás, J.; Viladiu, P. *Tumor Biol.* **2003**, *24*, 209–218.
- (45) Pastor, A.; Menendez, R.; Cremades, M. J.; Pastor, V.; Llopis, R.; Aznar, J. *Eur. Respir. J.* **1997**, *10*, 603–609.
- (46) Rapellino, M.; Niklinski, J.; Pecchio, F.; Furman, M.; Baldi, S.; Chyczewski, L.; Ruffini, E.; Chyczewska, E. *Eur. Respir. J.* **1995**, *8*, 407–410.
- (47) Takada, M.; Masuda, N.; Matsuura, E.; Kusunoki, Y.; Matui, K.; Nakagawa, K.; Yana, T.; Tuyuguchi, I.; Oohata, I.; Fukuoka, M. *Br. J. Cancer* **1995**, *71*, 160–165.
- (48) Foa, P.; Fornier, M.; Miceli, R.; Seregini, E.; Santambrogio, L.; Nosotti, M.; Cataldo, I.; Sala, M.; Caldiera, S.; Bombardieri, E. *Anticancer Res.* **1999**, *19*, 3613–3618.
- (49) Lee, H. J.; Kim, Y. T.; Park, P. J.; Shin, Y. S.; Kang, K. N.; Kim, Y.; Kim, C. W. *J. Thorac. Cardiovasc. Surg.* **2012**, *143*, 421–427.
- (50) Park, S. Y.; Lee, J. G.; Kim, J.; Park, Y.; Lee, S. K.; Bae, M. K.; Lee, C. Y.; Kim, D. J.; Chung, K. Y. *Lung Cancer* **2013**, *79*, 156–160.
- (51) Angenendt, P. *Drug Discovery Today* **2005**, *10*, S03–S11.
- (52) Joos, T. O.; Stoll, D.; Templin, M. F. *Curr. Opin. Chem. Biol.* **2002**, *6*, 76–80.
- (53) Templin, M. F.; Stoll, D.; Schrenk, M.; Traub, P. C.; Vohringer, C. F.; Joos, T. O. *Drug Discovery Today* **2002**, *7*, 815–822.
- (54) Wilson, D. S.; Nock, S. *Angew. Chem., Int. Ed.* **2003**, *42*, 494–500.
- (55) Medintz, I. L.; Uyeda, H. T.; Goldman, E. R.; Mattoussi, H. *Nat. Mater.* **2005**, *4*, 435–446.
- (56) Cheng, M. M. C.; Cuda, G.; Bunimovich, Y. L.; Gaspari, M.; Heath, J. R.; Hill, H. D.; Mirkin, C. A.; Nijdam, A. J.; Terracciano, R.; Thundat, T.; Ferrari, M. *Curr. Opin. Chem. Biol.* **2006**, *10*, 11–19.
- (57) Olmsted, I. R.; Kussrow, A.; Bornhop, D. J. *Anal. Chem.* **2012**, *84*, 10817–10822.
- (58) Mandrekar, S. J.; Sargent, D. J. *J. Clin. Oncol.* **2009**, *27*, 4027–4034.
- (59) Mandrekar, S. J.; Sargent, D. J. *J. Biopharm. Stat.* **2009**, *19*, 530–542.
- (60) Sawyers, C. L. *Nature* **2008**, *452*, 548–552.



- (61) Criqui, M. H.; Ho, L. A.; Denenberg, J.; Knoke, J. D.; Ninomiya, J. K.; Brehm, E. A.; McDermott, M. M.; Ridker, P. M. *Circulation* **2003**, *107*, E7026–E7027.
- (62) Ridker, P. M.; Buring, J. E.; Cook, N. R. *N. Engl. J. Med.* **2003**, *348*, 1060–1061.
- (63) Ridker, P. M.; Buring, J. E.; Rifai, N.; Cook, N. R. *JAMA, J. Am. Med. Assoc.* **2007**, *297*, 1433–1433.
- (64) Erbel, R.; Budoff, M. *Eur. Heart J.* **2012**, *33*, 1201–1213.
- (65) Lepor, H.; Cheli, C. D.; Thiel, R. P.; Taneja, S. S.; Laze, J.; Chan, D. W.; Sokoll, L. J.; Mangold, L.; Partin, A. W. *Bju Int.* **2012**, *109*, 1770–1775.